JACS
JOURNAL OF THE AMERICAN CHEMICAL SOCIETY

Article

pubs.acs.org/JACS

Room Temperature Phosphorescence of Metal-Free Organic Materials in Amorphous Polymer Matrices

Dongwook Lee,[†] Onas Bolton,[‡] Byoung Choul Kim,[†,∥] Ji Ho Youk,[⊥] Shuichi Takayama,[†,∥,#] and Jinsang Kim*[,†,‡,§,∥]

[†]Macromolecular Science and Engineering, [‡]Department of Materials Science and Engineering, and [§]Department of Chemical Engineering, 2300 Hayward St., University of Michigan, Ann Arbor, Michigan 48109, United States

[∥]Department of Biomedical Engineering, 2200 Bonisteel Blvd., University of Michigan, Ann Arbor, Michigan 48109, United States

[⊥]Department of Advanced Fiber Engineering, Division of Nano-Systems Engineering, Inha University, Incheon, 402-751, Korea

[#]Division of Nano-Bio and Chemical Engineering WCU Project, UNIST, Ulsan, Korea

ABSTRACT: Developing metal-free organic phosphorescent materials is promising but challenging because achieving emissive triplet relaxation that outcompetes the vibrational loss of triplets, a key process to achieving phosphorescence, is difficult without heavy metal atoms. While recent studies reveal that bright room temperature phosphorescence can be realized in purely organic crystalline materials through directed halogen bonding, these organic phosphors still have limitations to practical applications due to the stringent requirement of high quality crystal formation. Here we report bright room temperature phosphorescence by embedding a purely organic phosphor into an amorphous glassy polymer matrix. Our study implies that the reduced beta (β)-relaxation of isotactic PMMA most efficiently suppresses vibrational triplet decay and allows the embedded organic phosphors to achieve a bright 7.5% phosphorescence quantum yield. We also demonstrate a microfluidic device integrated with a novel temperature sensor based on the metal-free purely organic phosphors in the temperature-sensitive polymer matrix. This unique system has many advantages: (i) simple device structures without feeding additional temperature sensing agents, (ii) bright phosphorescence emission, (iii) a reversible thermal response, and (iv) tunable temperature sensing ranges by using different polymers.

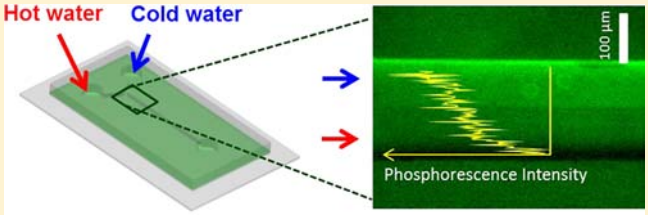

INTRODUCTION

Phosphorescent materials have attracted much attention due to potential applications in display, solid state lighting, optical storage and sensors because they can theoretically realize threefold higher internal quantum efficiency than fluorescent alternatives by harvesting triplet excitons through intersystem crossing.[1−4] There are two critical processes in photoluminescent (PL) phosphorescence: (i) spin flipping from an excited singlet state to a triplet state and (ii) radiative decay from the excited triplet state to the ground state. Many organometallic compounds are efficient phosphors since both processes are promoted by spin−orbit coupling present in metals.[5,6] While these materials exhibit high quantum efficiency, they require rare and expensive elements such as platinum and iridium. In contrast, purely organic phosphorescent compounds are cheaper but generally weaker and relatively rare because they exhibit long-lived triplets that are easily consumed by vibrational effects, preventing emissive decay. Thus, one of the challenges that organic compounds must overcome in order to become competitive with organometallic phosphors is finding a way to suppress vibration in order to achieve bright emission.

Aromatic ketones such as benzophenone are well-known phosphorescent materials that have been studied for several decades.[7] Excited state electrons in aromatic ketones cross from S_1 to T_2 at very high efficiency because of strong spin−orbit coupling and triplet T_2 levels that are often close in energy to S_1.[8] This spin−orbit coupling is localized at the carbonyl oxygen.[9] Because of this, aromatic ketones are an attractive moiety for designing metal-free organic phosphors. In order for the triplet to survive long enough for phosphorescence, vibrational dissipation from T_1 to the ground state must be suppressed as it competes with phosphorescent decay. Adequately suppressing vibration is perhaps the most important and challenging aspect of achieving efficient organic phosphorescence at room temperature.

Yuan et al. observed purely organic phosphorescence from benzophenone and its halogenated derivatives by growing crystals in common organic solvents.[10] Moreover, Bolton et al. developed color-tunable organic phosphorescence materials by implementing a directed heavy atom effect with halogen atoms also in crystalline systems.[11] In this material design, strong halogen bonding between the oxygen atom of an aromatic carbonyl and bromine promotes spin−orbit coupling and suppresses vibrational dissipation at the same time by the strict order of the crystal states of the materials. Though these

Received: February 18, 2013
Published: March 25, 2013

 © 2013 American Chemical Society dx.doi.org/10.1021/ja401769g | J. Am. Chem. Soc. 2013, 135, 6325−6329

approaches are very promising for developing metal-free organic phosphors, they still have limitations to practical applications because they stringently require crystalline materials.[12] Film forming materials, such as polymers and amorphous solids, would be more attractive for device fabrication and processing; however, a means must be found to induce in these systems vibrational suppression that is on par with that generated by crystals.

Herein we report our systematic investigation to deconvolute the suppression of the vibrational dissipation from the spin−orbit coupling enhancement by embedding a purely organic triplet-generating small molecule into a glassy polymer film and demonstrate bright metal-free organic phosphorescence from amorphous materials. The polymer serves as a rigid matrix to suppress vibration in the small molecule phosphor, as would a crystal, and thus allows the long-living triplets of the organic compound to survive long enough to emit. This phenomenon was studied using a single phosphorescent compound in various glassy polymer matrixes. We systematically investigated the correlation between the emission intensity of the embedded organic phosphors and physicochemical properties of the matrix polymers. Our study reveals that solubility parameter matching between the phosphorescent compound and the polymer matrix is a critical requirement to achieve a well-mixed embedding of the chromophore into the polymer and facilitate emission. Also, phosphorescence efficiency is strongly dependent on polymer tacticity because each arrangement exhibits a different degree of β-relaxation, which greatly affects the vibrational dissipation of the excited state triplets. This lifts the stringent crystalline requirement for metal-free organic phosphorescence materials and provides more process-friendly medium and a more physically tunable matrix.

We also demonstrated the use of amorphous purely organic phosphor films as a temperature sensor in a microfluidic device. Accurate temperature control is essential in such devices as they are often used for biological applications.[13] In this application, organic phosphors have many advantages over other conjugated polymer-based temperature sensors: (i) simple device structures, that is, no need for additional inlet to feed temperature sensing agents, (ii) brighter emission from phosphorescence as compared with polydiacetylene (PDA)-based fluorescence, (iii) a wholly reversible thermal response, and (iv) tunable temperature sensing ranges by using different polymer. This is the first example showing metal-free organic phosphorescence in an amorphous material, demonstrating its attractiveness as a temperature sensor in microfluidic devices. Moreover, we expect that this system can also be utilized in other biomedical applications due to the biocompatibilities of each component. Furthermore, developing appropriate conducting polymers as a glassy matrix for the organic phosphorescence materials may realize bright, color tunable, and flexible phosphorescent organic light emitting diodes as well.

RESULTS AND DISCUSSION

The weakly emitting organic phosphor, 2,5-dihexyloxy-4-bromobenzaldehyde (Br6A, Figure 1a), was embedded into atactic poly(methyl methacrylate) (aPMMA) resulting in a thin film with green phosphorescence. Alone, microcrystalline films of Br6A produce very weak emission that is largely dominated by the weak blue fluorescence of the compound seen at 425 nm. In films the phosphorescent quantum yield of Br6A increased from essentially zero to detectable level of 0.7% at

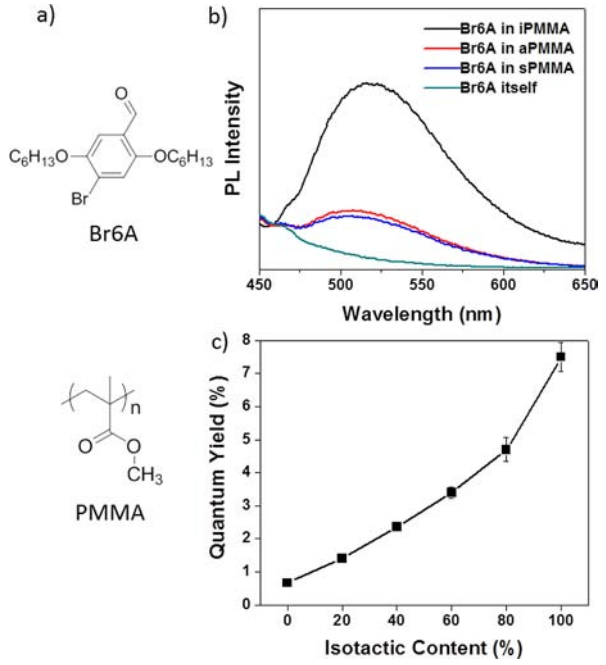

Figure 1. (a) Structure of a phosphor (Br6A) and polymer (PMMA). (b) PL emission spectra of Br6A and Br6A embedded in iPMMA, aPMMA and sPMMA. (c) Phosphorescence quantum yield with various isotactic content. The excitation wavelength was 365 nm.

room temperature. The increase in phosphorescent emission at 520 nm from the polymer film is evidence that the PMMA is acting to suppress vibration and enhance emissive triplet relaxation (Figure 1b). Assuming that a more well-ordered rigid polymer would restrict vibration even more efficiently, we tested polymers with higher degrees of crystallinity such as polypropylene (PP) and poly(hexamethylene adipamide) (Nylon 6/6). However, the quantum yield for these films was below our detection limit (<0.1%) for both cases. We believe that this is because the solubility parameter of these polymers (16.0 $MPa^{1/2}$ and 27.8 $MPa^{1/2}$, respectively) does not match with that of the phosphor (18.8 $MPa^{1/2}$) and, thus, the phosphor does not become sufficiently embedded into these polymer films. As a result, the phosphor molecules do not get the benefit of the polymer rigidity and are not emissive due to vibrational dissipation. On the contrary, PMMA has a solubility parameter of 19.0 $MPa^{1/2}$ that is similar to that of the phosphor, indicating that the phosphor is well mixed into that polymer matrix.

Notably, we found that the quantum efficiency of Br6A in PMMA strongly depends on polymer tacticity. Br6A embedded in isotactic PMMA (iPMMA) shows 10-fold brighter phosphorescence at room temperature than the same amount of Br6A in aPMMA or syndiotactic PMMA (sPMMA), as shown in Figure 1b. Indeed, as the relative amount of iPMMA present in the host polymer increases from 0 to 100% an exponential trend is observed as the quantum efficiency climbs from 0.7 to 7.5% (Figure 1c). This is attributed to the β-relaxation behavior of these polymers. β-Relaxation is considered to be the onset of motions that initiate the long-range segmental motions occurring at T_g.[14] In PMMA, this is caused by the onset of rotation of the ester side group, appearing around 285−300 K.[15] The intensity of the β-relaxation in amorphous PMMA increases with increasing syndiotacticity but decreases with increasing isotacticity.[16]

dx.doi.org/10.1021/ja401769g | J. Am. Chem. Soc. 2013, 135, 6325−6329

Dominant β-relaxation in aPMMA and sPMMA means there is independent motion of the carbonyl dipole in the ester side group. As the isotacticity increases, the β loss peak vanishes, indicating that the carbonyl dipole motion is locked. The rotation energy was calculated by using Allinger "MM2" force field model, showing that the rotating side group of iPMMA must force the two adjacent ester groups to undergo torsional oscillations of $\pm 16^{\circ}$ to relieve the stress during rotation of the central group leading to more activation energy (110 kJ mol^{-1}) than aPMMA (80 kJ mol^{-1}) and sPMMA (91 kJ mol^{-1}).[15]

Figure 2 shows the effect of β-relaxation. As sample temperatures decrease, phosphorescence intensity increases.

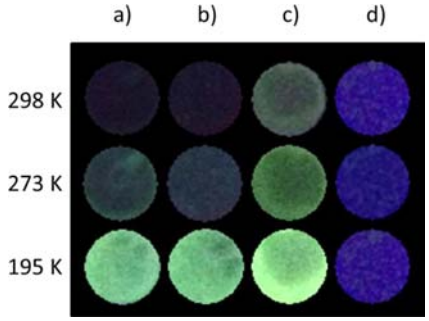

Figure 2. Phosphorescence emission of Br6A embedded in (a) aPMMA, (b) sPMMA, and (c) iPMMA at different temperatures. (d) Blue fluorescence emission of pure Br6A visible in part due to a lack of green phosphorescence also at these temperatures. The excitation wavelength was 365 nm.

The previously reported rigidity spectra show that the most significant β-relaxation appears around at 300 K and decreases with decreasing temperature.[17] We can see bright emission at lower temperatures from samples on ice (273 K) or on dry ice (195 K). However, even when the temperature is dropped to 195 K, the phosphor itself (not in PMMA) does not emit brightly, as shown in Figure 2d where only the inherent deep-blue fluorescence of Br6A is visible, which is indicative of disordered chromophores.[11] From these observations, we hypothesize that phosphorescence efficiency is dependent on the degree of β-relaxation and, thus, can be enhanced by lowering temperature, which restricts β-relaxation.

An optimum phosphor concentration was found to be 1 wt % versus polymer mass as shown in Figure 3a. At high concentrations of phosphor, self-quenching is expected and is believed to cause the observed low emission. At very low concentrations, there is much less opportunity for molecules of

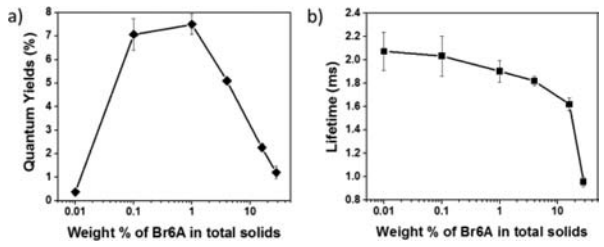

Figure 3. (a) Phosphorescence quantum yield at different phosphor concentrations for Br6A embedded in iPMMA. (b) Phosphorescence lifetime at different phosphor concentrations. Samples were annealed at 90 °C for 20 min. The excitation wavelength was 365 nm, and lifetime was monitored by the emission wavelength at 520 nm.

Br6A to find one another and realize the emission enhancing benefits of halogen bonding. So, though the aforementioned solubility parameter matching indicates that a high degree of miscibility is required to achieve adequate phosphor/polymer mixing, this result suggests that phosphor molecules can also suffer from too much isolation/mixing, indicating that some phosphor contact is necessary to achieve phosphorescence. At lower concentrations, as the concentration increases the chance for the halogen bonding increases, resulting in more efficient heavy atom effect and halogen bonding. To prove this hypothesis, we measured the phosphorescence lifetime of various concentrations of Br6A mixed into PMMA. As the phosphor concentration increases, the phosphorescent quantum yield increases, indicating that more halogen bonding facilitates intersystem crossing. Increasing halogen bonding up to a 1 wt % mixing ratio made radiative decay more dominant, resulting in high quantum yield and relatively short lifetime. But at higher concentrations nonradiative self-quenching dominates over radiative decay, the overall radiative rate decreases, and quantum yield falls faster than lifetime does.

In this study, we found solubility parameter matching and suppressing β-relaxation to be key components to reduce vibrational loss of phosphor triplets. Also, bright phosphorescence was realized by choosing a proper polymer matrix, iPMMA, and optimized mixing ratio between an organic phosphor and a polymer matrix. Moreover, we expect that this system can be utilized in organic light emitting diodes if a phosphor is embedded in appropriate conducting polymers as a glassy matrix.

This novel amorphous phosphorescence is strongly dependent on ambient temperature so that it can be useful as a temperature sensor. Accurate temperature measurements are difficult but critical in microfluidic devices performing biological processes such as polymerase chain reaction (PCR), temperature gradient focusing (TGF), and enzyme-activated reactions.[18−22] PDA-based conjugated polymers have been recently demonstrated as potential microfluidic temperature sensors by reporting fluorescent intensities correlated to the temperature of the PDA droplet.[13] Composite blends of PDA and a proper polymer matrix enable reversible fluorescence by increasing the stability of the PDAs.[23,24] However, the PDA must be kept separate from the reaction mixture and complicated channel structure must be used to make an additional inlet to feed PDA molecules. Polymer-based microfluidic devices feature low manufacturing costs and can be made from a wider range of materials that can be tailored for specific applications, as opposed to glass or silicon.[25] Polymers such as PMMA are popular construction materials for such microfluidic devices due to good processability, chemical resistance against acids and oils, and low cost.[26−28] Coining in situ temperature sensing in devices made from such a material would, ideally, not compromise the attractive qualities of the polymer, be easy to incorporate without the need of new device structure, and be economically on par with low-cost plastics.

While organometallic phosphors exhibit high quantum efficiency they are often, due to the short lifetimes of their triplets, relatively unaffected by temperature changes in the biologically relevant 30−60 °C range.[29,30] Also the vibrational freedoms of crystalline systems are largely unaffected by noncryogenic temperature changes below their melting points, making them poor near-ambient temperature sensors in their crystalline forms. However, embedding similar organic phosphor compounds into more temperature-sensitive ma-

dx.doi.org/10.1021/ja401769g | J. Am. Chem. Soc. 2013, 135, 6325−6329

trices, such as polymers, offers the possibility of enhancing the effect of temperature on phosphorescent emission intensity in ways that can be exploited for temperature sensing. Thus, these PMMA films of purely organic phosphors were explored as sensitive, inert, and cheap temperature sensors. As the sample temperature approaches the glass transition point of iPMMA, 55 °C, phosphorescence intensity decreases nearly linearly. As is shown in Figure 4, this creates a dramatic and predictable change in emission intensity across the temperature range of approximately 30−60 °C.

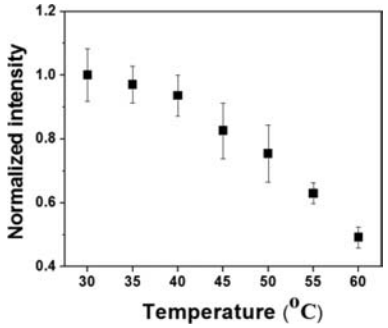

Figure 4. Normalized emission intensities for Br6A embedded in iPMMA at different temperatures excited at 365 nm.

The in situ phosphorescence spectra in a heating and cooling cycle in the temperature range of 30−60 °C was recorded in order to monitor thermal response reversibility. Faster decreases in phosphorescent intensity as temperature increases with relatively slower increases in phosphorescent intensity as temperature decreases were observed (Figure 5a). Incomplete intensity recovery seen in the first cooling cycle is probably ascribed to residual transitional motion of the fresh polymer occurring at higher temperatures. Following the first heating, reversible phosphorescence was repeated in six consecutive cycles, indicating that temperature sensing in microfluidic devices using this system can be reusable (Figure 5b).

In Figure 6 is demonstrated a microfluidic device composed of a polydimethylsiloxane (PDMS) channel on a glass slide coated with Br6A embedded in iPMMA. The microchannel device was soaked in a hot water bath heated to 60 °C to reduce the phosphorescence emission intensity from the device. Next, hot (60 °C) and cold (4 °C) water was supplied through two separate inlets into the microchannel to generate laminar flow inside the channel with a thermal gradient induced at the boundary. As shown in the fluorescence microscope image and the inserted graph, due to the temperature gradient created across the 200 μm wide channel, the phosphorescence emission intensity increases linearly from the side of the channel having hot water to the cold side of the channel.

■ CONCLUSIONS

In summary, we have realized efficient phosphorescence at room temperature by embedding a purely organic phosphor, Br6A, into glassy PMMA matrices. The activation of phosphorescence is likely due to fairly efficient restriction of vibrational decay due to the rigidity of the polymer matrix. Through systematic investigation we found that the tacticity of PMMA strongly affects quantum efficiency of the embedded organic phosphors. Our study implies that the reduced β-relaxation of iPMMA most efficiently suppresses the vibrational decay and allows the embedded organic phosphors to achieve a

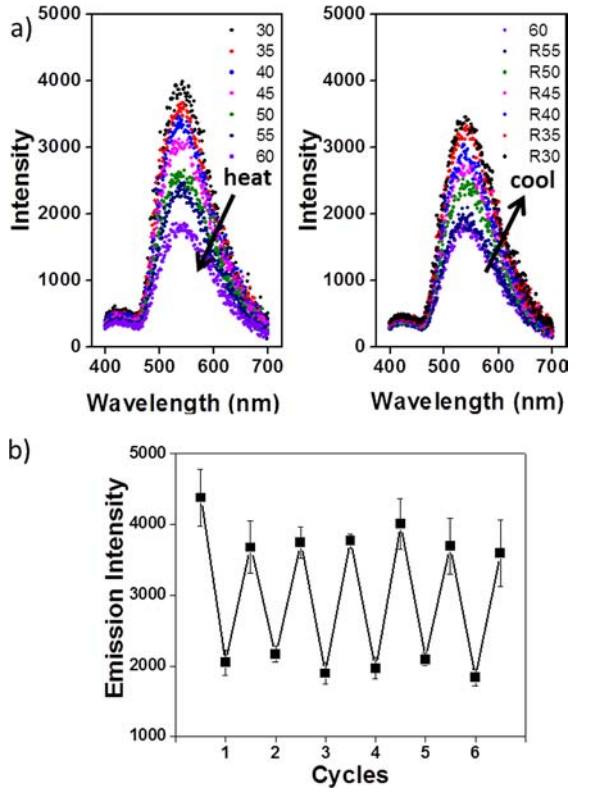

Figure 5. (a) In situ phosphorescence spectra in a heating and cooling cycle in the temperature range of 30−60 °C. (b) In situ phosphorescence intensities during six cycles. The excitation wavelength was 365 nm.

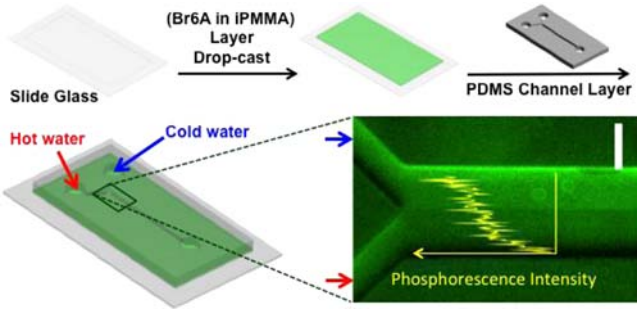

Figure 6. Schematic fabrication process and operation of a microfluidic device composed of a phosphorescence layer (Br6A in iPMMA) and a PDMS channel layer. Phosphorescence emission intensity under 365 nm UV light increases linearly from the hot side of the channel to the cold side channel. Scale bar = 100 μm.

bright 7.5% phosphorescence quantum yield. We also demonstrated a novel temperature sensor based on metal-free organic phosphorescence which is established by embedding a phosphor in a glassy polymer matrix, iPMMA. Organic phosphors are useful here because emission from the long-lived triplets they generate is dictated by vibrational suppression in the temperature-sensitive polymer matrix. This unique system has many advantages over conjugated polymer-based alternatives. This is also the first example showing amorphous metal-free organic phosphorescence, which is uniquely practical as a temperature sensor in microfluidic devices. We expect that this system can be especially useful in biomedical applications due to biocompatibilities of each component.

dx.doi.org/10.1021/ja401769g | J. Am. Chem. Soc. 2013, 135, 6325−6329

EXPERIMENTAL SECTION

Materials. iPMMA (Aldrich, M_w = 120 kg/mol), sPMMA (Aldrich, M_w = 996 kg/mol), aPMMA (Aldrich, M_w = 15 kg/mol), PP (Aldrich, M_w = 174 kg/mol), and poly(hexamethylene adipamide) (Nylon 6/6, Aldrich) were used as polymer matrix without further purification. 2,2,2-Trifluoroethanol (Aldrich) and toluene (Aldrich) were used as solvents for Nylon 6/6 and PP, respectively, without further purification. An organic phosphor, Br6A, was synthesized following previously reported synthetic routes.[11]

Solubility Parameter Calculation. Solubility parameter of Br6A was calculated by group contribution method.[31] The dispersive, polar, and hydrogen-bonding parameters from the Hoftyzer and van Krevelen's table were used by simple additive rules. Hildebrand parameter of PP, poly(hexamethylene adipamide) (Nylon 6/6) and PMMA was used to estimate polymer's solubility parameter.[32]

PL and QY Measurement. PL emission, excitation and quantum yield (QY) were collected using a Photon Technologies International (PTI) Quantamaster system equipped with an integrating sphere. Samples for quantum yield measurement were prepared by dropping mixed solution with chloroform onto an unmodified glass substrate followed by annealing at 90 °C for 20 min. Absorption and emission inside the sphere were determined by comparison to a blank sample (glass only). A neutral density filter was used to allow for maximization of the emission signal without saturating the photomultiplier tube detector with excitation light. Each sample type was run in quadruplicate with each quantum yield measurement coming from a freshly drop cast sample. Measurements proved highly repeatable, and errors are given as ±1 standard deviation.

Microfluidic Device Preparation. A "Y" shaped microchannel structure was fabricated using a conventional soft lithography technique. A transparent mask (CAD Art Inc.) bearing the channel pattern was transferred to SU-8 (Microchem Inc.) deposited on a silicon wafer. A 10:1 mixture of PDMS (Sylgard 184, Dow corning) and curing agent was poured onto the mold and cured at 60 °C for at least 4 h before use. Phosphorescent layer was prepared by homogeneously drop casting 100:1 mixture of iPMMA and Br6A on a slide glass followed by annealing at 90 °C for 20 min. Afterward, the PDMS layer and the phosphorescence layer were bonded together by plasma treatment (COVANCE-MP, Femto-science Inc.). The microchannel device was soaked in a hot water bath, heated up to 60 °C to reduce the emitted light intensity from the device. Then hot (60 °C) and cold (4 °C) water was supplied through two separate inlets into the microchannel to generate laminar flow inside the channel with a thermal gradient induced at the boundary. Emitted light intensity from the device was measured by a fluorescence microscope (Ti, Nikon).

Temperature Dependent Emission Measurement. Emitted light intensity from a film of 100:1 mixture of iPMMA and Br6A was measured using a plate reader (BioTeck Synergy Neo plate reader) under controlled temperature conditions. Repetitive measurements of the emission were conducted to record the cyclic intensity changes between high temperature and low temperature conditions.

AUTHOR INFORMATION

Corresponding Author

jinsang@umich.edu

Notes

The authors declare no competing financial interest.

ACKNOWLEDGMENTS

We acknowledge the financial support from National Science Foundation (CAREER Award DMR 0644864). D.L. was partly supported by a fellowship from LG Chemical, Korea.

REFERENCES

(1) Tang, C. W.; VanSlyke, S. A. *Appl. Phys. Lett.* **1987**, *51*, 913−915.

(2) Baldo, M. A.; O'Brien, D. F.; You, Y.; Shoustikov, A.; Sibley, S.; Thompson, M. E.; Forrest, S. R. *Nature* **1998**, *395*, 151−154.

(3) Adachi, C.; Baldo, M. A.; Forrest, S. R.; Thompson, M. E. *Appl. Phys. Lett.* **2000**, *77*, 904−906.

(4) You, Y.; Han, Y.; Lee, Y.-M.; Park, S. Y.; Nam, W.; Lippard, S. J. *J. Am. Chem. Soc.* **2011**, *133*, 11488−11491.

(5) Lamansky, S.; Djurovich, P.; Murphy, D.; Abdel-Razzaq, F.; Lee, H.; Adachi, C.; Burrows, P. E.; Forrest, S. R.; Thompson, M. E. *J. Am. Chem. Soc.* **2001**, *123*, 4304−4312.

(6) Niu, Y.; Tung, Y.; Chi, Y.; Shu, C.; Kim, J. H.; Chen, B.; Luo, J.; Carty, A. J.; Jen, A. K. *Chem. Mater.* **2005**, *17*, 3532−3536.

(7) Kearns, D. R.; Case, W. A. *J. Am. Chem. Soc.* **1966**, *88*, 5087−5097.

(8) Kiritani, M.; Yoshii, T.; Hirota, N.; Baba, M. *J. Chem. Phys.* **1994**, *98*, 11265−11268.

(9) Klessinger, M.; Michl, J. *Excited States and Photochemistry of Organic Molecules*; VCH Publishers: New York, 1995; pp 266−271.

(10) Yuan, W. Z.; Shen, X. Y.; Zhao, H.; Lam, J. W. Y.; Tang, L.; Lu, P.; Wang, C.; Liu, Y.; Wang, Z.; Zheng, Q.; Sun, J. Z.; Ma, Y.; Tang, B. Z. *J. Phys. Chem. C* **2010**, *114*, 6090−6099.

(11) Bolton, O.; Lee, K.; Kim, H.-J.; Lin, K. Y.; Kim, J. *Nat. Chem.* **2011**, *3*, 205−210.

(12) Kabe, R.; Lynch, V. M.; Anzenbacher, P., Jr. *CrystEngComm* **2011**, *13*, 5423−5427.

(13) Ryu, S.; Yoo, I.; Song, S.; Yoon, B.; Kim, J.-M. *J. Am. Chem. Soc.* **2009**, *131*, 3800−3801.

(14) Mark, J. E., Ed. *Physical Properties of Polymers Handbook*; Springer: New York, 2007, pp 217−232.

(15) Cowie, J. M. G.; Ferguson, R. *Polymer* **1987**, *28*, 503−508.

(16) Gillham, J. K.; Boyer, S. J. R. F. *Polymer* **1976**, *17*, 996−1008.

(17) Gillham, J. K.; Stadnicki, S. J. *J. Appl. Polym. Sci.* **1977**, *21*, 401−424.

(18) Lagally, E. T.; Medintz, I.; Mathies, R. A. *Anal. Chem.* **2001**, *73*, 565−570.

(19) Mao, H.; Yang, T.; Cremer, P. S. *J. Am. Chem. Soc.* **2002**, *124*, 4432−4435.

(20) Ross, D.; Gaitan, M.; Locascio, L. E. *Anal. Chem.* **2001**, *73*, 4117−4123.

(21) Ross, D.; Locascio, L. E. *Anal. Chem.* **2002**, *74*, 2556−2564.

(22) Kim, S. M.; Sommer, G. J.; Burns, M. A; Hasselbrink, E. F. *Anal. Chem.* **2006**, *78*, 8028−8035.

(23) Lee, S.; Lee, J.; Kim, H. N.; Kim, M. H.; Yoon, J. *Sens. Actuators, B* **2012**, *173*, 419−425.

(24) Wang, X.-D.; Song, X.-H.; He, C.-Y.; Yang, C. J.; Chen, G.; Chen, X. *Anal. Chem.* **2011**, *83*, 2434−2437.

(25) Becker, H.; Locascio, L. E. *Talanta* **2002**, *56*, 267−287.

(26) Henry, A. C.; Tutt, T. J.; Galloway, M.; Davidson, Y. Y.; McWhorter, C. S.; Soper, S. A.; McCarley, R. L. *Anal. Chem.* **2000**, *72*, 5331−5337.

(27) McCormick, R. M.; Nelson, R. J.; Alonso-Amigo, M. G.; Benvegnu, D. J.; Hooper, H. H. *Anal. Chem.* **1997**, *69*, 2626−2630.

(28) Becker, H.; Heim, U. *Sens. Actuators, A* **2000**, *83*, 130−135.

(29) Borisov, S. M.; Wolfbeis, O. S. *Anal. Chem.* **2006**, *78*, 5094−5101.

(30) Borisov, S. M.; Vasylevska, A. S.; Krause, C.; Wolfbeis, O. S. *Adv. Funct. Mater.* **2006**, *16*, 1536−1542.

(31) Brandrup, J., Immergut, E. H., Grulke, E. A., Eds. *Polymer Handbook*; Wiley-Interscience, New York, 1999; pp 682−686.

(32) Barton, A. F. M. *Handbook of Polymer-Liquid Interaction Parameters and Solubility Parameters*; CRC Press: Boca Raton, FL, 1990; pp 265−284.